

## Research Article

## Plasma-Activated Municipal Wastewater (PAMW): Revolutionizing Municipal Wastewater into High-Value Liquid Fertilizer for Duckweed Cultivation through Air Plasma Treatment

Sunisa Ungwiwatkul, Mathin Jaikua, Kanyarak Prasertboonyai and Phuthidhorn Thana\*

Faculty of Science, Energy and Environment, King Mongkut's University of Technology North Bangkok, Rayong Campus, Rayong, Thailand

Arlee Tamman

Thailand Institute of Nuclear Technology (Public Organization), Nakhon Nayok, Thailand

Khanit Matra\*

Department of Electrical Engineering, Faculty of Engineering, Srinakharinwirot University, Nakhon Nayok, Thailand

\* Corresponding author. E-mail: phuthidhorn.t@sciee.kmutnb.ac.th; khanit@g.swu.ac.th

DOI: 10.14416/j.asep.2025.04.002

Received: 10 May 2024; Revised: 6 June 2024; Accepted: 25 June 2024; Published online: 23 April 2025

© 2025 King Mongkut's University of Technology North Bangkok. All Rights Reserved.

### Abstract

This study investigates the potential of pin-to-water surface atmospheric pressure air plasma-activated municipal wastewater (PAMW), driven by solar energy, for cultivating duckweed (*Lemna minor* L.). By capitalizing on the essential macronutrients, especially phosphate, inherent in the wastewater, the research aims to create a cost-effective source of plant nutrients. The air plasma treatment not only efficiently purifies the wastewater but also yields vital nitrogen fertilizer, particularly nitrate and ammonium, at no extra cost. The optimal 1.00 cm discharge gap in a plasma-electrolysis reactor with three anode modules maximizes the reduction of the chemical oxygen demand (COD) in PAMW. The treatment significantly degrades contaminants, notably reducing COD values, with the longest treatment time (30 min) producing the highest nitrite, nitrate, ammonium and hydrogen peroxide content— $87.00 \pm 0.46$  mg/L,  $54.72 \pm 0.66$  mg/L,  $6.62 \pm 0.06$  mg/L and  $69.98 \pm 0.66$  mg/L, respectively. Under these optimal conditions, duckweed cultivation in PAMW exhibits substantial growth, increasing biomass by 6.4 times in 7 days. Crude protein rises from 12.52 % of dry weight (DW) to 33.06 % DW, carotenoid content increases from  $1346.12 \mu\text{g g}^{-1}$  DW to  $2816.11 \mu\text{g g}^{-1}$  DW, and total chlorophyll grows from  $4.26 \text{ mg g}^{-1}$  DW to  $10.40 \text{ mg g}^{-1}$  DW. The COD of PAMW significantly decreases from 138.67 mg/L to 48.00 mg/L. These findings propose a cohesive and cost-effective approach to the sustainable cultivation of duckweed and other plants using enhanced PAMW.

**Keywords:** Duckweed cultivation, Plasma-activated municipal wastewater (PAMW), Plasma-water-based nitrogen fixation, Wastewater treatment

### 1 Introduction

Regarding the increasing world population, this causes many consequences, including pollution management and food shortages due to the improper environment, pollution, and climate change. Moreover, the shortage of energy due to the limited fossil fuels could affect

the quality of life, especially in remote areas [1], [2]. Therefore, in addressing these issues, it is imperative to deliberate upon methods for enhancement and prevention.

Duckweeds, which are aquatic green plants in the Lemnaceae family, have been used as potential nutrient absorbers from wastewater, primarily nitrogen



and phosphorus [3]. Duckweeds cultivated in sewage have been effectively utilized as a replacement for soybean meal and fish meal, comprising up to 15% of the poultry diet, resulting in favorable outcomes such as enhanced egg production and increased yolk production [4]. Regarding the content of macro- and micro-nutrients including high crude protein content, amino acids, carbohydrates, vitamins, minerals, and pigments like beta-carotene and xanthophylls, duckweeds have been proposed as a promising candidate for animal feed as well as future human food [4]–[6]. Moreover, duckweeds have been proven to be a promising biofuel production feedstock as well as efficient CO<sub>2</sub> sequestration due to their rapid growth, high starch content, and relatively low lignin content [7]–[10]. However, to implement large-scale production of duckweed cultivation, the challenge of the capital cost of fertilizer and wastewater management must be considered.

Currently, plasma-activated water (PAW) or plasma-treated water (PTW) technology has been applied in various fields, including food, agriculture, medicine, and water treatment, regarding its green merits and unique characteristics without causing secondary pollution [11]–[17]. The reactive oxygen species (ROS) generated in water during exposure to plasma can be used in wastewater treatment, known as the cold atmospheric plasma-based advanced oxidation processes (AOPs). The generated ROS by plasma has high oxidation potential, and they can react and eliminate many pollutants in wastewater at low temperatures without additional hazardous chemicals. Plasma-based AOPs for wastewater treatment can be used to remove a variety of pollutants contaminated in wastewater, such as dyes, pharmaceuticals, surfactants, personal care products [12], [18]–[20], and microorganisms including bacteria, fungi, and viruses [21]–[23]. Additionally, complex chemicals and compounds like phenols, 2,4,6-trinitrophenol, phencyclidine, dioxins, and pesticides could be also probably broken down by plasma-based AOPs [24], [25].

The degradation of contaminants through plasma treatment occurs via AOPs that are induced by the presence of powerful oxidizing agents. Of the oxidizers produced by the interaction between plasma and liquid, the hydroxyl radical (OH) is the most reactive species among the plasma-generated ROS [26]. Hydroxyl radicals have a broad range of reactivity and an outstanding capacity to oxidize, which make them a potential option for breaking down different organic and inorganic substances present in

wastewater into carbon dioxide, water, and inorganic ions [27], [28]. The other ROS commonly presented in PAW include atomic oxygen (O), ozone (O<sub>3</sub>), hydrogen peroxide (H<sub>2</sub>O<sub>2</sub>), and hydroperoxyl radical (HO<sub>2</sub>). These ROS are highly effective oxidizing agents with greater oxidation potentials than chlorine frequently and chemically used in wastewater treatment [12], [29]–[31]. In addition, the interaction between atmospheric plasma and water also results in the production of liquid nitrogen fertilizer, specifically nitrate (NO<sub>3</sub><sup>-</sup>) and ammonium (NH<sub>4</sub><sup>+</sup>), which is referred to as plasma-water-based nitrogen fixation [32]–[35]. This technology offers a sustainable and environmentally friendly nitrogen fixation process that promotes energy efficiency and can be easily implemented for distributed production. Importantly, it can be operated under atmospheric conditions [36]–[38].

In this study, plasma-activated municipal wastewater (PAMW) has been proposed as a medium for duckweed (*Lemna minor* L.) cultivation. In order to support the green sustainable campaign of Thailand, including the Sustainable Development Goals (SDG), climate change adaptation, and advancing “net-zero” energy processes towards a bio-circular-green (BCG) economy, a strategic move involves harnessing municipal wastewater as a pivotal water source for the production of PAMW in the cultivation of duckweed. The focal objective lies in harnessing the advantages of municipal wastewater to generate PAMW. By incorporating AOPs during plasma treatment, not only can the municipal wastewater be effectively purified, but also vital plant primary macronutrients—nitrogen (N), phosphorus (P), and potassium (K)—can be derived from key components such as urea (CH<sub>4</sub>N<sub>2</sub>O), ammonium (NH<sub>4</sub><sup>+</sup>), phosphate (PO<sub>4</sub><sup>3-</sup>), and potassium ion (K<sup>+</sup>). These constituents present in municipal wastewater originating from human and animal waste, food waste, as well as specific soaps and detergents, serve to address a notable limitation of PAW, which primarily offers nitrogen compounds. This multifaceted approach ensures a more comprehensive and balanced nutrient supply for enhanced agricultural applications [39]–[43]. The economical and energy-sustained atmospheric DC plasma model (pin-to-water surface) has been designed for the plasma-electrolysis-based treatment of wastewater. The treatment system has been intentionally decided to operate within the quasi-closed system in order to enhance the production of H<sub>2</sub>O<sub>2</sub> and NO<sub>3</sub><sup>-</sup>, which are mostly generated via the reaction in the gas phase (vaporized water) [24], [44], [45]. The generation of

plasma has been driven by renewable solar energy harvested by a solar panel. To verify the possibility of a practical large-scale production, the number of plasma model units has been varied. The physicochemical attributes of the generated PAMW from municipal wastewater have been assessed in order to investigate the influence of the plasma-electrolysis-based treatment on especially  $\text{H}_2\text{O}_2$ ,  $\text{NO}_2^-$ ,  $\text{NO}_3^-$ , and  $\text{NH}_4^+$  production, as well as on the originally present  $\text{PO}_4^{3-}$  within municipal wastewater. The optimally generated PAMW has been subsequently applied as a source of nutrients for duckweed cultivation. The investigation of selected nutritional parameters in PAMW and their impact on duckweed growth has been conducted. Additionally, the electrical and optical characteristics of the plasma were observed and analyzed.

## 2 Materials and Methods

### 2.1 Plasma model and electrical measurement

Figure 1 shows the schematic representation of the experimental configuration for plasma-electrolysis-based treatment of domestic sewage. The experimental setup employed a DC discharge plasma generator in a pin-to-liquid electrode configuration. Three tungsten anode pins (diameter of 1.0 mm, tip diameter of 0.1 mm) surrounded a 316 L stainless steel cathode (diameter of 3.0 mm). The entire system was housed within a closed container equipped with a gas exchange port (diameter of 1.0 cm). The distance from each anode electrode to the cathode rod was set to 2 cm. The immersion depth of the mutual cathode under the water surface was 10 cm, while the tip of each anode was located above the water surface. The discharge gaps (DG) between anode tips could be varied in the range of 0.25–1.00 cm.

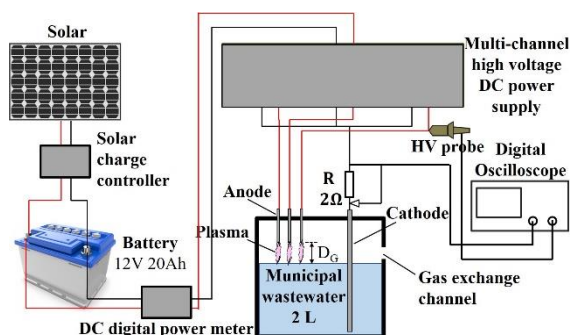


**Figure 1:** Schematic diagram of the experimental setup for domestic wastewater treatment with the plasma-electrolysis reactor.

The plasma-electrolysis reactor was driven by a multi-channel high-voltage direct current (DC) power supply. Each independent module in the power source is made up of a flyback transformer and a zero-voltage-switching (zvs) flyback driver, and it can generate up to 10 kV. The high-voltage generator was powered by a 240 W off-grid solar power system that comprises a solar panel, a solar charge controller, and a battery. The average electrical power dissipated in a plasma discharge was calculated from the following Equation (1):

$$\overline{P} = (1/T) \int_0^T V(t)I(t)dt \quad (1)$$

where  $T$  is the period of the voltage waveform. The instantaneous discharge voltage across the electrodes  $V(t)$  was measured using a high-voltage probe (P6015A; Tektronix, Inc., United States; 75 MHz bandwidth), while the discharge current  $I(t)$  was deduced from measuring the voltage drop across a  $2\Omega$  monitor resistor using another high-voltage probe (Hantek PP-200; Qingdao Hantek Electronic Co., Ltd., China; 200 MHz bandwidth). The V-I waveforms were recorded using a digital oscilloscope (Hantek DSO2C15; Qingdao Hantek Electronic Co., Ltd., China; 150 MHz bandwidth with 1 GSa/s sampling rate). The total electric power consumed by the system of a multi-channel high-voltage DC generator was measured using a DC digital power meter (PZEM 031; Ningbo Peacefair Electronic Technology Co., Ltd., China).

## 2.2 Optical emission spectra measurement

The plasma-produced species in the plasma-active region were observed using optical emission spectroscopy (OES) equipped with a compact wide-range spectrometer (Exemplar LS; B&W Tek, United States), which covers the range between 200–900 nm with a spectral resolution of 0.4 nm. The light emission from the band of hydroxyl (OH) radical was detected by a high-resolution spectrometer with 0.05 nm resolution (AvaSpec-ULS3648, Avantes, the Netherlands), and the spectrum ranging from 265 to 335 nm was measured. The optical emission was collected at about 2.0 cm away from the plasma discharge zone and all collected spectra were plasma volume-averaged. All spectra were averaged for 5 samplings per measurement to increase the signal-to-noise ratio.



### 2.3 Quantitative measurement of PAMW

All chemicals used were analytical reagent grade. The concentration of hydrogen peroxide ( $\text{H}_2\text{O}_2$ ) in PAMW was determined by redox titration using potassium permanganate ( $\text{KMnO}_4$ ), and the chemical oxygen demand (COD) in sewage was measured using the closed reflux method according to standard methods for the examination of water and wastewater [46].

The concentrations of nitrite ( $\text{NO}_2^-$ ), nitrate ( $\text{NO}_3^-$ ), ammonium ( $\text{NH}_4^+$ ), and phosphate ( $\text{PO}_4^{3-}$ ) in PAMW were analyzed by spectrophotometry. A colored complex was formed by the reaction between the appropriate chemical reagents and the target substance. A UV-Vis spectrophotometer (UV-2600; Shimadzu Corporation, Japan) was used for measuring the absorption spectra of each color-complex compound at a particular wavelength. Nitrite content in wastewater samples was determined using Saltzman's reagent and measured at a maximum absorption wavelength of 540 nm [47]. Nitrate content in wastewater samples was determined by measuring the first-derivative of the spectrometric spectrum of nitrosalicylic acid in the basic solution formed by the nitration reaction of salicylic acid under highly acidic conditions at the maximum wavelength at 410 nm [48]. Phosphate in wastewater samples was determined by using the phosphomolybdic acid method and measuring at a maximum wavelength of 880 nm [49]. For the ammonium analysis, PAMW samples were measured via the indophenol blue colorimetric method [50]. All measurements were performed at least three times.

The pH value of PAMW was analyzed using a pH meter (S220K, Mettler Toledo, Switzerland). Before determination, the pH meter was calibrated with 4.0, 7.0, and 10.0 buffer solutions. Electrical conductivity (EC) was measured with a conductivity meter (CON700, Eutech, Singapore) at an ambient temperature of 25 °C.

### 2.4 Municipal wastewater resource

All domestic wastewater was sampled from the municipal wastewater treatment plant of Ban Phe subdistrict municipality, Mueang Rayong district, Rayong province, Thailand. Municipal wastewater samples, following physical treatments at the wastewater treatment plant, exhibited very low levels of suspended solids and turbidity. Each 2 L of domestic sewage from the same lot of sampled water

will be treated by a plasma-electrolysis reactor, analyzed, and subsequently applied for duckweed cultivation. The untreated domestic wastewater contains  $\text{NO}_3^-$ , with a concentration of  $0.55 \pm 0.02$  mg/L;  $\text{NH}_4^+$ , with a concentration of  $4.81 \pm 0.03$  mg/L; and  $\text{PO}_4^{3-}$ , with a concentration of  $0.47 \pm 0.03$  mg/L. While  $\text{NO}_2^-$  was detected in small amounts around  $0.20 \pm 0.05$  mg/L. The COD of untreated domestic sewage, which is an indicator of the amount of organic matter and other oxidizable pollutants dissolved in wastewater, was approximately  $138.67 \pm 2.31$  mg/L. This COD value exceeds Thailand's standard COD value for industrial wastewater of 120 mg/L. Electrical conductivity (EC) and pH of untreated municipal wastewater were  $761.67 \pm 0.58$   $\mu\text{S}/\text{cm}$  and  $7.20 \pm 0.01$ , respectively. There was no  $\text{H}_2\text{O}_2$  in the wastewater before plasma treatment.

### 2.5 Plant material and growth conditions of duckweed cultivation in PAMW

The duckweed, *Lemna minor* L., used for this study was collected from a pond located in Nong La Lok, Ban Khai District, Rayong, Thailand ( $12^\circ 48' 00.2''\text{N}$   $101^\circ 13' 50.5''\text{E}$ ). The plant was cultured in 4 L of a plastic container with 0.1 g/L of NPK 15:15:15 fertilizer and acclimatized for 3 days. Next, 3 grams of the initial wet weight of duckweed were placed in the plastic container (40 cm  $\times$  26 cm  $\times$  13 cm), which contained 2 L of PAMW, with plasma treatment times of 0 (untreated), 10, 15, 20, 25, and 30 min. The pH was adjusted to 6.5 via the addition of 1.0 M NaOH and 1.0 M HCl. All experiments were conducted in triplicate, and the plastic containers were placed in a greenhouse constructed of insect net walls and a translucent polycarbonate roof for 7 days under 50% solar irradiation. After 7 days of cultivation, the plants were harvested and gently washed with tap water. The samples were dried to a constant weight in an oven at 80 °C and weighed to obtain the dry weight.

### 2.6 Determination of chlorophyll and carotenoid contents

The total chlorophyll contents and carotenoid contents of the duckweed cultured with untreated wastewater and PAMW were determined following the method of Kundu *et al.* [51]. 0.2 g of dried duckweed was placed in the mortar and crushed in 10 mL of 80% aqueous acetone. The supernatant was collected by centrifugation for 10 min at 5,000 rpm, and the process was repeated

for the precipitate or pellet. The absorbance of the solution was measured using spectrophotometry at wavelengths of 470 nm, 645 nm, and 663 nm.

## 2.7 Estimation of protein content

The crude protein content was estimated by measuring nitrogen content ( $N \times 6.25$ ) by the Kjeldahl method as described by method 991.20 of the official methods of analysis of AOAC International [52].

## 2.8 Statistical analysis

All assays were performed in three replicates. The data were analyzed using IBM SPSS Statistics 28 software. Statistical analysis was performed using a one-way analysis of variance (ANOVA). The significance of differences between pairs of group means was determined by Tukey's honestly significant difference (Tukey's HSD) test. Data with  $p$ -values smaller than 0.05 ( $p$ -value  $< 0.05$ ) were considered statistically significant. The data were reported as mean values, and standard deviations (SDs) from three replicates in each experiment were reported.

# 3 Results and Discussion

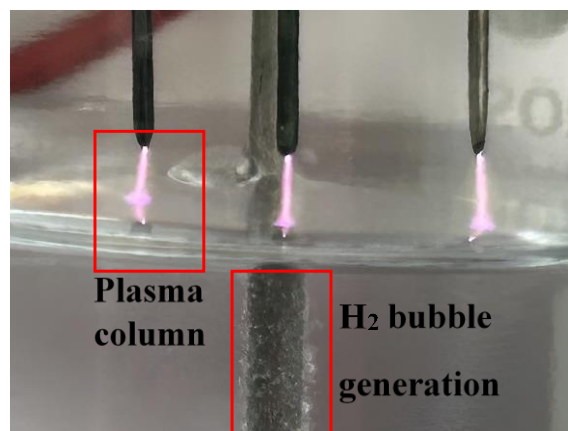
## 3.1 Plasma and electrical characteristics

Figure 2(a) shows an example image of the electrical discharges above the domestic wastewater at a 1-cm discharge gap between the pin anode and water surface. The visual plasma character is a uniform bright purple-glow plasma column with a size around  $\varnothing$  1.1 mm slightly larger than the anode diameter. During the treatment, hydrogen ( $H_2$ ) gas bubble productions could be noticed around the surface of the stainless-steel rod immersed under the treated wastewater cathode by the reduction of half-reaction of water. The wastewater plant's pretreatments reduced the suspended solids and turbidity in municipal wastewater samples. As a result, the plasma-electrolysis system produced minimal sludge, allowing for easy separation from the wastewater through gravity settling.

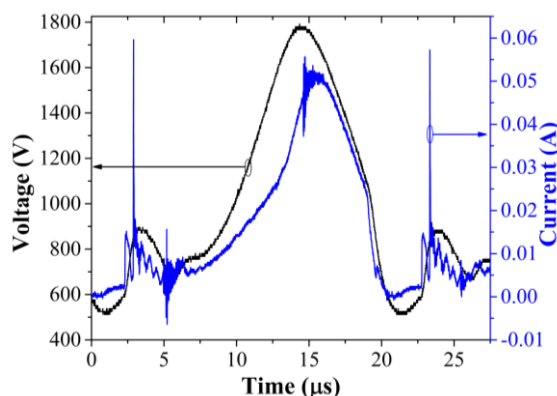
The time-synchronized waveform of the discharge current ( $I$ ) and voltage ( $V$ ) for a plasma discharge in the plasma-electrolysis reactor with an anode and a discharge gap of 1 cm is depicted in Figure 2(b). Though the contact DC voltage was utilized, the discharge current was performed in a DC self-pulsing discharge [53], [54]. This could imply that

the plasma was in the mode of spark-to-glow discharge [15], [54], [55]. The repetition rate of the discharge pulse was around 50 kHz. For discharge gaps of 0.25 cm, 0.50 cm, and 1.00 cm, the pulse-average electrical powers dissipated in a plasma discharge with a single anode were  $21.2 \pm 0.7$  W,  $23.4 \pm 0.5$  W, and  $26.1 \pm 0.8$  W.

At the same time, the system of the multi-channel DC power supply consumed a total electric power of  $64.9 \pm 0.6$  W,  $66.0 \pm 0.8$  W, and  $69.8 \pm 0.6$  W, respectively. The electric power consumed by the multi-channel DC power supply for a discharge gap of 1.00 cm was  $142.1 \pm 1.0$  W and  $211.6 \pm 0.5$  W, respectively, when the number of anodes was 2 and 3, respectively.



(a)

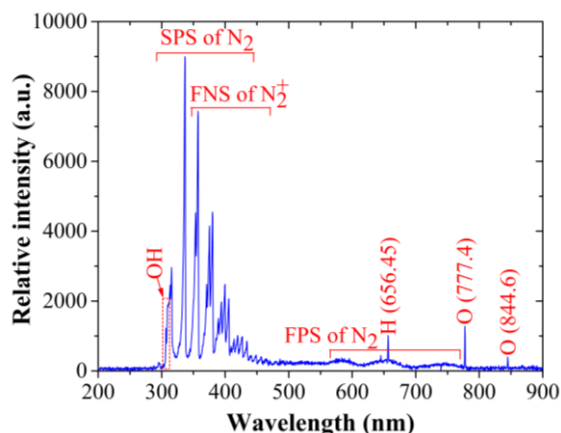


(b)

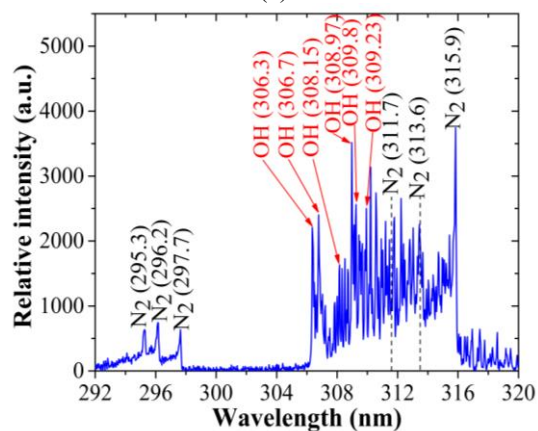
**Figure 2:** (a) The plasma column and hydrogen bubble generation and (b) the V–I characteristics of a single discharge pulse in the plasma-electrolysis reactor with 1-anode plasma discharge and 1-cm discharge gap.

### 3.2 Optical emission characteristics

The observed emission spectra of the plasma generated in the plasma-electrolysis reactor with an anode and the discharge gap of 1 cm during domestic wastewater treatment are shown in Figure 3(a).



(a)



(b)

**Figure 3:** (a) The broadband optical emission spectra and (b) the hydroxyl (OH) radical emission spectrum of the plasma generated in the plasma-electrolysis reactor with an anode and a discharge gap of 1 cm during domestic wastewater treatment.

The dominant radiation spectra of the second positive system (SPS) of  $N_2$  ( $C^3\Pi_u \rightarrow B^3\Pi_g$ ) and the first negative system (FNS) of  $N_2^+$  ( $B^2\Sigma_u^+ \rightarrow X^2\Sigma_g^+$ ) were observed in the wavelength range of 295 – 449 nm and 355–471 nm, respectively [56]. The emission spectrum of hydroxyl radical generated in the plasma-electrolysis is shown in Figure 3(b). It clearly showed

that light emitted in the wavelength range of 306 – 312 nm was emitted from the OH radicals ( $A^2\Sigma^+ \rightarrow X^2\Pi_i, 0-0$  band) [57]. Meanwhile, the emission spectrum of the OH ( $A^2\Sigma^+ \rightarrow X^2\Pi_i, 1-1$ ) band in the wavelength around 312–316 nm was interfered with by the emission spectrum of  $\Delta v = +1$  the vibration transition band of  $N_2$  ( $C^3\Pi_u \rightarrow B^3\Pi_g$ ) [58], [59]. Further, the emission band of the first positive system (FPS) of  $N_2$  ( $B^3\Pi_g \rightarrow A^3\Sigma_u^+$ ) was also seen in the wavelength range of 580–773 nm [60], [61]. In addition, the emission lines of atomic hydrogen ( $H_\alpha$ , 656.45 nm) and oxygen (O, 777.4 and 844.6 nm) were also seen.

### 3.3 PAMW characteristics generated by plasma-electrolysis system

#### 3.3.1 Number of independent anodes with power source module dependence

Regarding the problem of large-scale production of PAMW, an array of plasma electrodes in the plasma reactor has been proposed as a solution. However, an increase in the plasma electrodes while the power source per plasma reactor has been fixed usually causes difficulty in controlling the uniformity of plasma generated from each electrode. Therefore, in this work, independent anodes with power source modules have been used in order to investigate the effect of the number of independent anodes with power source module dependence on the concentration of chemicals in domestic wastewater treated with the plasma-electrolysis reactor. The atmospheric pressure plasma in the plasma-electrolysis reactor was generated by changing the number of anode modules. The plasma treatment time and the discharge gap were set at 10 min and 1.00 cm, respectively. Figure 4(a) shows that the concentration of nitrite increased significantly from  $0.20 \pm 0.05$  mg/L (untreated) to  $27.50 \pm 0.47$  mg/L,  $39.62 \pm 0.97$  mg/L, and  $59.55 \pm 1.00$  mg/L after plasma treatment with the different numbers of anode modules of 1, 2, and 3, respectively. Similarly, with increasing the number of anode modules from 1 to 3 anodes, the content of nitrate increased significantly from  $0.55 \pm 0.02$  mg/L (untreated) to  $10.03 \pm 0.74$  mg/L,  $13.78 \pm 0.73$  mg/L, and  $18.42 \pm 0.57$  mg/L, respectively, as well as the concentration of hydrogen peroxide increased significantly from  $0.00 \pm 0.00$  mg/L (untreated) to  $5.98 \pm 0.12$  mg/L,  $12.51 \pm 0.43$  mg/L, and



18.21±0.29 mg/L, respectively. The concentration of ammonium in municipal wastewater increased from 4.81±0.03 mg/L (untreated) to 5.15±0.08 mg/L, 5.38±0.07 mg/L, and 5.48±0.07 mg/L corresponding to the number of anode modules increased from 1 to 3, respectively, as shown in Figure 4(b).

In contrast to other chemicals, the amount of phosphate in PAMW slightly decreased from 0.47±0.03 mg/L (untreated) to 0.36±0.01 mg/L, 0.35±0.01 mg/L, and 0.34±0.02 mg/L after exposure to plasma generated with 1 to 3 anode modules, respectively. As shown in Figure 4(c), with increasing the number of anode modules from 1 to 3, the EC of the PAMW significantly increased from 761.67±0.58 µS/cm (untreated) to 764.00±3.61 µS/cm, 771.67±3.21 µS/cm, and 787.33±2.52 µS/cm, respectively; meanwhile, the pH significantly decreased from 7.20±0.01 (untreated) to 6.83±0.03, 6.67±0.05, and 6.34±0.02, respectively. Figure 4(d) shows that the COD of municipal wastewater dropped significantly from 138.67±2.31 mg/L (untreated) to 98.67±2.31 mg/L, 94.67±2.31 mg/L, and 84.00±4.00 mg/L, which corresponds to the number of anode modules increased from 1 to 3, respectively.

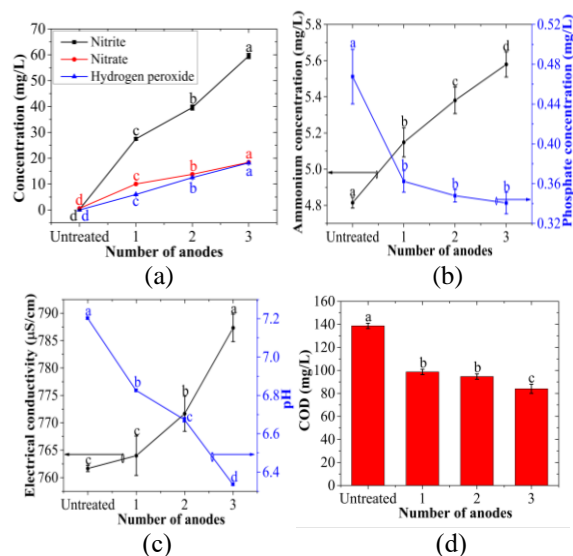


**Figure 4:** The effect of the number of anode modules on the selected parameters of municipal wastewater after being exposed to the atmospheric pressure plasma generated in the plasma-electrolysis reactor generated with a discharge gap of 1.00 cm and an exposure time of 10 min: (a) the concentrations of nitrite ( $\text{NO}_2^-$ ), nitrate ( $\text{NO}_3^-$ ), and hydrogen peroxide ( $\text{H}_2\text{O}_2$ ); (b) the concentrations of ammonium ( $\text{NH}_4^+$ )

and phosphate ( $\text{PO}_4^{3-}$ ); (c) the electrical conductivity (EC) and the pH, and (d) the chemical oxygen demand (COD). Error bars represent the SD of the mean with n=3. Different letters above or under the error bars indicate significant differences at the 0.05 level (one-way ANOVA and Tukey's HSD test).

### 3.3.2 Gap dependence

In order to investigate the effect of the discharge gap on the concentration of chemicals in municipal wastewater treated with the plasma-electrolysis reactor, the atmospheric pressure plasma in the plasma-electrolysis reactor was operated for PAMW generation with a variation of discharge gaps for 10 min treatment time, while the optimal number of anode modules from the previous section was fixed at 3 anode modules. After the domestic wastewaters were exposed to the plasma generated in the plasma-electrolysis reactor, the concentrations of nitrite, nitrate, and hydrogen peroxide dissolved in the PAMW strongly increased with the increased discharge gap, as shown in Figure 5(a). When the discharge gap increased from 0.25 cm to 0.50 cm and 1.00 cm (the maximum gap that plasma could be generated by the supplied voltage from a power source), the concentration of nitrate raised significantly from 0.55±0.02 mg/L (untreated) to 9.52±0.29 mg/L, 15.92±0.24 mg/L, and 18.44±0.43 mg/L, respectively; the concentration of nitrite grew significantly from 0.20±0.05 mg/L (untreated) to 27.67±0.62 mg/L, 31.26±0.89 mg/L, and 58.84±0.56 mg/L, respectively; the content of hydrogen peroxide increased significantly from 0.00±0.00 mg/L (untreated) to 11.63±0.04 mg/L, 15.75±0.04 mg/L, and 17.89±0.10 mg/L, respectively. The concentration of ammonium increased slightly from 4.81±0.03 mg/L (untreated) to 5.28±0.06 mg/L, 5.48±0.06 mg/L, and 5.55±0.18 mg/L, respectively, as depicted in Figure 5(b). In contrast to ammonium, the amount of phosphate decreased slightly from 0.47±0.03 mg/L (untreated) to 27.67±0.62 mg/L, 31.26±0.89 mg/L, and 58.84±0.56 mg/L after treatment of plasma generated with discharge gaps from 0.25 cm to 0.50 cm and 1.00 cm, respectively. Figure 5(c) shows that with increased gap discharge from 0.25 cm to 0.50 cm and 1.00 cm, the electrical conductivity of PAMW increased from 763.00±1.00 µS/cm (untreated) to 765.33±3.79 µS/cm, 774.67±2.52 µS/cm, and 786.33±3.51 µS/cm, respectively, while the pH decreased from 7.20±0.01 (untreated) to 6.91±0.01, 6.55±0.01, and 6.35±0.01, respectively. The COD

value of PAMW decreased significantly from  $138.67 \pm 2.31$  mg/L (untreated) to  $101.33 \pm 2.28$  mg/L,  $93.33 \pm 2.35$  mg/L, and  $85.33 \pm 2.31$  mg/L, corresponding to the increased discharge gap from 0.25 to 0.50 cm and 1.00 cm, as shown in Figure 5(d).

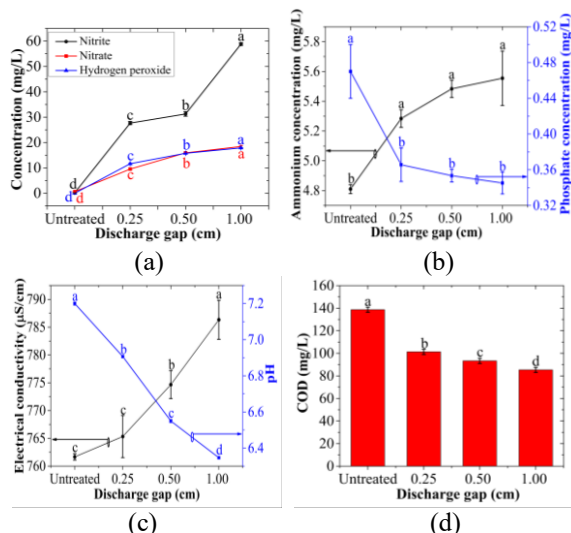


**Figure 5:** The effect of the discharge gaps on the selected parameters of domestic wastewater after being exposed to the atmospheric pressure plasma generated in a plasma-electrolysis reactor generated with 3 anode modules and an exposure time of 10 min: (a) the concentrations of nitrite ( $\text{NO}_2^-$ ), nitrate ( $\text{NO}_3^-$ ), and hydrogen peroxide ( $\text{H}_2\text{O}_2$ ); (b) the concentrations of ammonium ( $\text{NH}_4^+$ ) and phosphate ( $\text{PO}_4^{3-}$ ); (c) the electrical conductivity (EC) and the pH; and (d) the chemical oxygen demand (COD). Error bars represent the SD of the mean with  $n=3$ . Different letters above or under the error bars indicate significant differences at the 0.05 level (one-way ANOVA and Tukey's HSD test).

### 3.3.3 Time dependence

Figure 6 shows the effect of the treatment time on the parameters of wastewater treated with plasma in a plasma-electrolysis reactor with 3 anode modules and an optimal discharge gap from the previous section of 1.00 cm. With increased plasma treatment time from 0 min (untreated) to 10 min, 15 min, 20 min, 25 min, and 30 min, the dissolved concentrations of nitrite, nitrate, hydrogen peroxide, ammonium, and phosphate are shown in Figure 6(a).

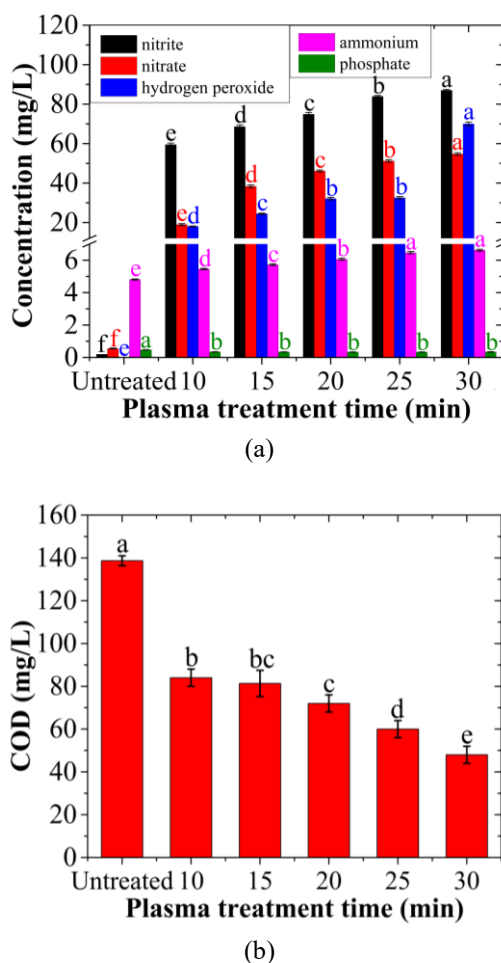


**Figure 6:** The effect of the plasma treatment times on the selected parameters of domestic wastewater after being exposed to the atmospheric pressure plasma generated in the plasma-electrolysis reactor with 3 anodes and a discharge gap of 1.00 cm: (a) the concentrations of nitrite ( $\text{NO}_2^-$ ), nitrate ( $\text{NO}_3^-$ ), hydrogen peroxide ( $\text{H}_2\text{O}_2$ ), ammonium ( $\text{NH}_4^+$ ), and phosphate ( $\text{PO}_4^{3-}$ ); and (b) the chemical oxygen demand (COD). Error bars represent the SD of the mean with  $n=3$ . Different letters above the error bars indicate significant differences at the 0.05 level (one-way ANOVA and Tukey's HSD test).

The content of nitrite increased significantly from  $0.20 \pm 0.05$  mg/L to  $59.46 \pm 0.76$  mg/L,  $68.59 \pm 0.89$  mg/L, and  $74.89 \pm 0.86$  mg/L,  $83.91 \pm 0.44$  mg/L, and  $87.00 \pm 0.46$  mg/L, respectively; the concentration of nitrate raised significantly from  $0.55 \pm 0.02$  mg/L to  $18.93 \pm 0.49$  mg/L,  $38.36 \pm 0.63$  mg/L,  $46.11 \pm 0.47$  mg/L,  $51.19 \pm 0.67$  mg/L, and  $54.72 \pm 0.66$  mg/L,



respectively; the amount of hydrogen peroxide grew significantly from  $0.00 \pm 0.00$  mg/L to  $18.02 \pm 0.20$  mg/L,  $24.44 \pm 0.31$  mg/L,  $32.10 \pm 0.35$  mg/L,  $32.51 \pm 0.61$  mg/L, and  $69.98 \pm 0.66$  mg/L, respectively. Similarly, the concentration of ammonium tended to increase from  $4.81 \pm 0.03$  mg/L, to  $5.46 \pm 0.04$  mg/L,  $5.72 \pm 0.05$  mg/L,  $6.06 \pm 0.07$  mg/L,  $6.46 \pm 0.07$  mg/L, and  $6.62 \pm 0.06$  mg/L with increasing plasma treatment time. On the contrary, the phosphate content in PAMW dropped from  $0.47 \pm 0.03$  mg/L to  $0.35 \pm 0.02$  mg/L,  $0.34 \pm 0.02$  mg/L,  $0.33 \pm 0.02$  mg/L,  $0.33 \pm 0.03$  mg/L, and  $0.34 \pm 0.03$  mg/L after exposure to plasma with plasma treatment times in the range of 0 to 30 min. The phosphate concentration decreased after plasma treatment, but there was no significant difference between treatments with different plasma treatment times. The pH of PAMW decreased significantly from  $7.21 \pm 0.02$  to  $6.35 \pm 0.02$ ,  $5.35 \pm 0.01$ ,  $3.92 \pm 0.01$ ,  $3.43 \pm 0.01$ ,  $3.22 \pm 0.02$ , corresponding to the increased plasma treatment time. Figure 6(b) depicts that the COD of PAMW treated with the plasma-electrolysis reactor significantly decreased from  $138.67 \pm 2.31$  mg/L (untreated) to  $84.00 \pm 4.00$  mg/L,  $81.33 \pm 6.11$  mg/L,  $72.00 \pm 4.00$  mg/L,  $60.00 \pm 4.00$  mg/L, and  $48.00 \pm 4.00$  mg/L after 10 min, 15 min, 20 min, 25 min, and 30 min of plasma treatment. Regarding these results, it could be confirmed that in the proposed study, the increase in the number of independent anode modules and treatment time could quasi-linearly enhance the properties of PAMW. Therefore, the PAMWs treated with different plasma treatment times were subsequently applied for duckweed cultivation to investigate the influence of selected parameters in PAMWs on duckweed growth.

### 3.4 Duckweed growth and its nutritional composition contents

Regarding experimental results, the optimal plasma-electrolysis reactor with 3 anode modules with a 1.00 cm gap distance was used for the generation of PAMW for duckweed cultivation at various treatment times (0 min, 10 min, 20 min, and 30 min). The pH of PAMW in each condition had been adjusted to 6.5 via the addition of 1.0 M NaOH and 1.0 M HCl before being used for duckweed cultivation. It should be noted that the pH adjustment has not affected the concentration of other selected parameters. In order to evaluate the growth of duckweed cultivated in PAMW, measurements were made of the weight of duckweed as well as its nutritional value, including crude protein,

chlorophyll, and carotenoid, in duckweed cultivated with the PAMW for 7 days.

The duckweed had an initial weight of 3 g before cultivation, which is equivalent to 0.13 g dry weight. The dry weight of duckweed cultured in PAMW with treatment times of 0 (untreated), 10 min, 15 min, 20 min, 25 min, and 30 min was  $0.850 \pm 0.020$  g,  $0.810 \pm 0.021$  g,  $0.820 \pm 0.015$  g,  $0.830 \pm 0.021$  g,  $0.840 \pm 0.021$  g, and  $0.086 \pm 0.015$  g, respectively, after 7 days of cultivation. These dry weights were not statistically significantly different. The results of this experiment showed that duckweed had a rapid growth rate, with biomass (measured in terms of dry weight) increasing around 6.4 times the initial biomass after cultivation for 7 days.

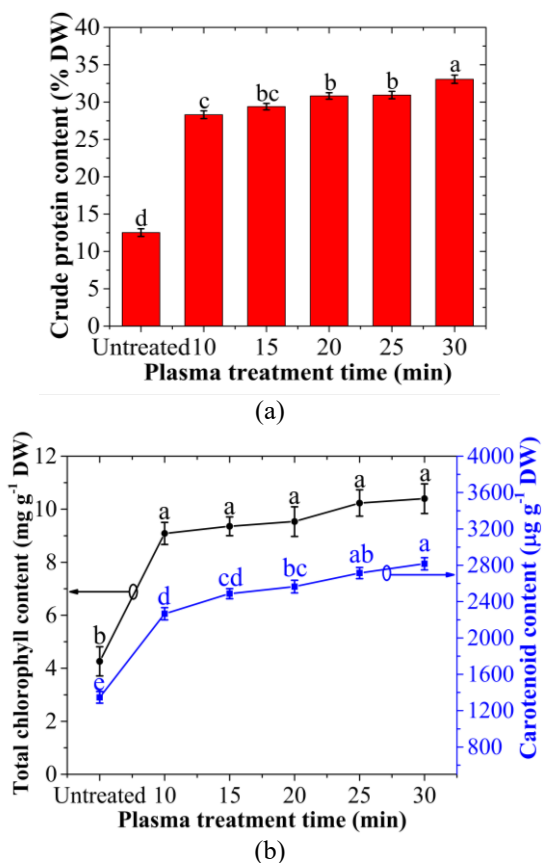


**Figure 7:** (a) Crude protein content (percent of dry weight (% DW)) and (b) total chlorophyll content ( $\mu\text{g g}^{-1}$  DW) and carotenoid content ( $\mu\text{g g}^{-1}$  DW) of the duckweed (*Lemna minor* L.) cultured in PAMW as a function of the plasma treatment time. The atmospheric pressure plasma generated in the plasma-electrolysis reactor was produced using 3 anodes and a discharge gap of 1.00 cm.

As shown in Figure 7(a), it was clear that the contents of crude protein in duckweed cultivated in PAMW increased significantly from  $12.52 \pm 0.51$  % of dry weight (DW) to  $28.31 \pm 0.52$  %DW,  $29.40 \pm 0.43$  %DW,  $30.83 \pm 0.43$  %DW,  $30.94 \pm 0.50$  %DW, and  $33.06 \pm 0.55$  % DW for a plasma treatment time of 0 min, 10 min, 15 min, 20 min, 25 min, and 30 min. Similarly, with increasing plasma treatment time, the carotenoid content of duckweed raised significantly from  $1346.12 \pm 64.37$   $\mu\text{g g}^{-1}$  of dry weight ( $\mu\text{g g}^{-1}\text{DW}$ ) to  $2265.93 \pm 66.85$   $\mu\text{g g}^{-1}\text{DW}$ ,  $2487.03 \pm 55.64$   $\mu\text{g g}^{-1}\text{DW}$ ,  $2564.97 \pm 69.83$   $\mu\text{g g}^{-1}\text{DW}$ ,  $2714.32 \pm 61.54$   $\mu\text{g g}^{-1}\text{DW}$ , and  $2816.11 \pm 66.83$   $\mu\text{g g}^{-1}\text{DW}$ , respectively, as depicted in Figure 7(b). The amount of total chlorophyll in duckweed cultivated in PAMW increased from  $4.26 \pm 0.55$   $\text{mg g}^{-1}\text{DW}$  to  $9.09 \pm 0.42$   $\text{mg g}^{-1}\text{DW}$ ,  $9.36 \pm 0.35$   $\text{mg g}^{-1}\text{DW}$ ,  $9.53 \pm 0.56$   $\text{mg g}^{-1}\text{DW}$ ,  $10.23 \pm 0.50$   $\text{mg g}^{-1}\text{DW}$ , and  $10.40 \pm 0.56$   $\text{mg g}^{-1}\text{DW}$ , which corresponds to plasma treatment time increasing from 0 min (untreated) to 10 min, 15 min, 20 min, 25 min, and 30 min, respectively.

However, total chlorophyll did not significantly differ with plasma treatment times.

The investigation has not only focused on the influence of PAMW on duckweed (*Lemna minor* L.) growth but has also examined the impact of selected nutritional parameters in PAMW on duckweed growth. The reduction in concentration of plant nutrients, namely nitrate, ammonium, and phosphate, was compared to their initial concentrations in the PAMW after 7 days of duckweed cultivation, as shown in Table 1. Duckweed grown in municipal wastewater treated with plasma for 30 min had the highest absorption of nitrate and ammonium from wastewater, at 28.01 mg/L (51.19% of the initial concentration) and 1.25 mg/L (18.81% of the initial concentration), respectively. Meanwhile, duckweed cultivated in untreated wastewater had the highest phosphate absorption from wastewater, around 0.41 mg/L (92.10% of the initial concentration). The result also reveals that the duckweed absorbed nitrogen nutrients in the form of nitrate more than ammonium.

**Table 1:** Depletion of plant nutrients in PAMWs after 7 days of duckweed (*Lemna minor* L.) cultivation. PAMWs were generated with different plasma activation times. ANOVA and Tukey's HSD tests show that data with different superscript letters within the same row are significantly different at the 0.05 level. The data are shown as the mean  $\pm$  SD of three separate experiments. Parentheses indicate the percentage of the plant nutrients reduced from their initial values.

Plant Nutrient	Plasma Treatment Time (min)					
	Untreated	10	15	20	25	30
$\text{NO}_3^-$	$0.24 \pm 0.01^f$ (44.94%)	$6.98 \pm 0.97^c$ (36.79%)	$18.57 \pm 0.90^d$ (48.42%)	$23.45 \pm 0.12^c$ (50.86%)	$25.83 \pm 0.97^b$ (50.47%)	$28.01 \pm 0.69^a$ (51.19%)
$\text{NH}_4^+$	$0.84 \pm 0.00^d$ (17.67%)	$1.13 \pm 0.00^c$ (20.76%)	$1.11 \pm 0.08^c$ (19.43%)	$0.98 \pm 0.03^c$ (16.23%)	$1.18 \pm 0.01^b$ (18.24%)	$1.25 \pm 0.01^a$ (18.81%)
$\text{PO}_4^{3-}$	$0.41 \pm 0.02^a$ (92.10%)	$0.30 \pm 0.02^b$ (87.22%)	$0.32 \pm 0.02^b$ (95.99%)	$0.31 \pm 0.05^b$ (91.97%)	$0.32 \pm 0.03^b$ (98.17%)	$0.34 \pm 0.02^b$ (98.79%)

### 3.5 Influence of plasma-electrolysis-based treatment on PAMW and duckweed cultivation

Regarding the experimental results, it could be confirmed that the proposed plasma-electrolysis-based treatment process could be an effective tool for plasma-water activation and be practically useful for duckweed cultivation.

Generating plasma above the liquid surface using a pin-to-water plane configuration with a liquid-grounded electrode is a simple and practical approach for activating wastewater [62]. The adoption of 316L stainless steel for the submerged cathode was based on its exceptional corrosion resistance. The anode selection involved the use of tungsten, a frequently employed substance in incandescent filaments and

welding electrodes due to its exceptional characteristics such as a high melting point, density, and mechanical strength, even under high temperatures [63], [64]. The electrode configuration and materials employed in this method imply its potential to ensure stability and achieve high performance over an extended period in applications involving the activation of municipal wastewater. The pin-to-plane electrode configuration has inherent scalability; therefore, this method can be easily adjusted for larger-scale wastewater treatment and activation by increasing the number of anodes in a multi-pin array.

The ensuing discussion and proposed mechanism regarding the impact of plasma-

electrolysis-based treatment on PAMW characteristics and duckweed cultivation are elaborated on as follows.

In the plasma-electrolysis reactor, a pin-to-water electrode configuration is used, where the liquid surface serves as the cathode. The irradiation of positive ions (such as  $H^+$ ,  $N_2^+$ ,  $O_2^+$ , and  $H_2O^+$ ) from the plasma to the liquid surface leads to the product of hydronium cations, which are the precursors for the production of OH and  $H_2O_2$  dissolved in bulk liquid [65], [66]. In the generation of atmospheric pressure plasma using a pin-to-water electrode configuration reactor, the liquid cathode performs much better than the liquid anode in producing OH and  $H_2O_2$  through plasma-water interactions [65], [67]. The other important reactive oxygen and nitrogen species can also be produced in the gas phase from the interactions of the air plasma-liquid cathode, including atomic oxygen (O), ozone ( $O_3$ ), atomic hydrogen (H), hydroperoxyl radical ( $HO_2$ ), nitric oxide (NO), nitrogen dioxide ( $NO_2$ ), nitrous acid ( $HNO_2$ ), and nitric acid ( $HNO_3$ ) [66], [68]. However, the transportation of some species, including O,  $O_3$ , NO, and  $NO_2$ , from the gas phase into water is limited due to their relatively low Henry's law solubility coefficients [68], [69].

Regarding the lifespans of chemical substances generated via plasma-water interaction, only the species  $H_2O_2$ ,  $HNO_2$ ,  $HNO_3$ ,  $HO_2$ ,  $O_3$ , and  $ONOOH$ , which have long lifespans, can accumulate in the bulk liquid. The other species have short lives and only occur in the region approximately a few nanometers below the gas-liquid interface. Following plasma treatment, the concentrations of  $H_2O_2$ ,  $HNO_2$ ,  $NO_2^-$ ,  $HNO_3$ , and  $NO_3^-$  remain constant. However, other long-lived species are either lost through reactions (such as  $HO_2$  and  $ONOOH$  within 10 seconds) or evaporate in the gas phase (as is the case with  $O_3$ , due to its low Henry's constant) [33], [69]. However, the dissolution of gaseous OH into bulk water is limited due to its short lifetime (half-lifetime ~ few hundred  $\mu s$ ) and relatively low Henry's law solubility coefficient [70]. Thus, hydroxyl radicals, which play a crucial role in the oxidative degradation of contaminants in bulk wastewater, were probably formed from reactions involving the decomposition of the long-lived species  $H_2O_2$  [24], [69]. In addition, the other highly reactive oxygen species generated by plasma-water interaction, especially O,  $O_3$ ,  $H_2O_2$ , and  $HO_2$ , which have oxidation potentials of 2.42 V, 2.07 V, 1.77 V, and 1.44 V, respectively, can react and eliminate many pollutants in wastewater through oxidation processes like hydroxyl radical [12], [24].

Among the plasma-produced reactive oxygen species (ROS), hydroxyl radical (OH) is probably the most important one. It is the strongest oxygen-based oxidizing agent, with a standard oxidation potential ( $E_{OH/H_2O}^0$ ) of 2.81 V [70]. Plasma discharge in contact with water can produce OH radicals in the gas phase. Hydroxyl radical occurring in atmospheric air plasma can be produced from the dissociation of water molecules induced by direct electron-collision ( $e + H_2O \rightarrow OH + H + e$ , threshold electron energy = 7 eV) [24], reactions of oxidaniumyl (oxoniumyl) ( $H_2O^+$ ) radical ( $H_2O^+ + H_2O \rightarrow OH + H_3O^+$ ), interaction with excited oxygen ( $O(^1D) + H_2O \rightarrow OH + OH$ ), and reaction of metastable molecular nitrogen  $N_2(A^3\Sigma_u^+)$  ( $N_2(A^3\Sigma_u^+) + H_2O \rightarrow OH + H + N_2$ ) [71]. The presence of water molecules in the discharge environment has a significant impact on the chemistry of the gas phase plasma, specifically affecting the concentrations of OH and  $H_2O_2$ . During discharge, water molecules are transferred from the surface of the liquid into the plasma phase as a result of ion bombardment causing sputtering, discharge-produced thermal heating causing evaporation, and the electric field inducing the emission of hydrated ions [66], [67], [72]. The ionization of water molecules inside the plasma leads to the generation of  $H_2O^+$  ( $e + H_2O \rightarrow H_2O^+ + 2e$ , threshold electron energy = 13 eV) [24]. Hydroxyl radical can also be formed by reactions of oxidaniumyl radical ( $H_2O^+ + e \rightarrow OH + H$ ;  $H_2O^+ + H^- \rightarrow OH + H_2$ ;  $H_2O^+ + OH^- \rightarrow H_2O + OH$ ) as well as reactions of hydronium ion ( $H_3O^+ + e \rightarrow OH + H_2$ ;  $H_3O^+ + H^- \rightarrow OH + H_2 + H$ ) [24], [72]. The dominant formation of hydrogen peroxide by hydroxyl radical recombination ( $OH + OH \rightarrow H_2O_2$ ) can occur in the gas, the liquid, or at the gas-liquid interface [44]. Moreover, the gaseous  $H_2O_2$  has a high solubility with Henry's law constants,  $h_{H_2O_2} = 1.96 \times 10^6$ , while the

OH radical has a lower solubility with  $h_{OH} = 620$  [45].

Plant nitrogen nutrition in the form of nitrate and ammonium can be produced through atmospheric plasma-water-based nitrogen fixation. Nitrite ( $NO_2^-$ ) and nitrate ( $NO_3^-$ ) are produced from gaseous nitrogen oxides ( $NO_x$ ) generated by atmospheric plasma. In the plasma and plasma-liquid interface region, nitric oxide (NO) is formed through the following reactions:  $N_2^* + O \rightarrow NO + N$ ;  $N_2 + O \rightarrow NO + N$ ;  $O_2 + N \rightarrow NO + O$ ; and  $N + OH \rightarrow NO + H$  where  $N_2^*$  is the excited nitrogen molecule [36], [73]. While, nitrogen dioxide ( $NO_2$ ) is formed through the reactions:  $NO + O \rightarrow$

$\text{NO}_2$  and  $\text{NO} + \text{OH} \rightarrow \text{NO}_2 + \text{H}$  [36], [74], [75]. When the nitrogen oxides come into contact with water,  $\text{NO}_2^-$  and  $\text{NO}_3^-$  are produced by the reactions:  $2\text{NO}_2 + \text{H}_2\text{O} \rightarrow \text{NO}_2^- + \text{NO}_3^- + 2\text{H}^+$ ;  $\text{NO} + \text{NO}_2 + \text{H}_2\text{O} \rightarrow 2\text{NO}_2^- + 2\text{H}^+$ ;  $2\text{NO}_2 + 2\text{H}_2\text{O} \rightarrow \text{HNO}_2 + \text{NO}_3^- + \text{H}_3\text{O}^+$ ; and  $2\text{NO}_2 + 3\text{H}_2\text{O} \rightarrow \text{NO}_2^- + \text{NO}_3^- + 2\text{H}_3\text{O}^+$  [36], [69].  $\text{NO}$  and  $\text{NO}_2$  react with  $\text{OH}$  to form  $\text{HNO}_2$  and  $\text{HNO}_3$  [69], [75].  $\text{HNO}_2$  and  $\text{HNO}_3$  dissolved in water partially split into  $\text{H}_3\text{O}^+$  and  $\text{NO}_2^-$  or  $\text{NO}_3^-$  ions, respectively [69]. The ammonium ion ( $\text{NH}_4^+$ ) is formed by the protonation of ammonia ( $\text{NH}_3$ ), which is formed through the series of reactions of nitrogen (N) and hydrogen (H) radicals: (i)  $\text{N} + \text{H} \rightarrow \text{NH}$ ; (ii)  $\text{NH} + \text{H} \rightarrow \text{NH}_2$ ; and (iii)  $\text{NH}_2 + \text{H} \rightarrow \text{NH}_3$  [37], [75]. Based on this information, the proposed treatment system has been intentionally designed to operate within a quasi-closed system to enhance the generation of  $\text{H}_2\text{O}_2$  and  $\text{NO}_3^-$ . The quasi-closed system facilitates the collection of vaporized  $\text{OH}^-$  and  $\text{NO}$ , primarily generated in the gas phase (vaporized water), enhancing the production of  $\text{H}_2\text{O}_2$  and  $\text{NO}_3^-$  (the key parameters for wastewater treatment and vital nutrients for duckweed growth in this study). Subsequently, the condensed and dissolved compounds reintegrate into the bulk liquid.

Regarding the experimental results, it could be confirmed that the concentrations of nitrite, nitrate, hydrogen peroxide, and ammonium via the proposed plasma-electrolysis treatment significantly increased, as shown in Figure 4(a) and (b). The main nitrogen species in the wastewater formed during the plasma exposure were  $\text{NO}_3^-$  and  $\text{NO}_2^-$ , with  $\text{NO}_2^-$  being the predominant compound. Figure 5(b) shows the ammonium level in PAMW was higher than before treatment; nevertheless, the ammonium content in wastewater treated with different discharge gaps was not significantly different. Conversely, phosphate content in PAMW decreased after treatment. However, similar to ammonium, variations in discharge gaps did not impart a statistically significant difference in the phosphate content of the treated water. Decreasing of phosphate ions after plasma treatment can occur because they can combine with one proton ( $\text{H}^+$ ) to form hydrogen phosphate ions ( $(\text{HPO}_4)^{2-}$ ), two protons to form dihydrogen phosphate ions ( $(\text{H}_2\text{PO}_4)^-$ ), or three protons to form phosphoric acid ( $\text{H}_3\text{PO}_4$ ) [76].

Regarding the experimental results, the pH of PAMW has decreased when the electrode gap, the number of anode modules, and treatment times. Similarly to the pH trend, the COD value of PAMW exhibited a decrease with the increase of the

aforementioned parameters. The decrease in COD value aligns with the increase in  $\text{H}_2\text{O}_2$  as shown in Figures 4(a), 5(a) and 6(a). Referring to Henry's law as previously discussed, it is anticipated that  $\text{H}_2\text{O}_2$  will predominantly exist as the soluble oxidizing agent in PAMW in this study, playing a pivotal role in improving wastewater quality. Through the process of hydrogen peroxide oxidation, refractory organic compounds in wastewater undergo decomposition. Consequently, hydrogen peroxide efficiently oxidizes both organic and inorganic pollutants, making a substantial contribution to the reduction of both COD and biochemical oxygen demand (BOD) [77]. Nevertheless, it is anticipated that other oxidizing agents produced through plasma-based advanced oxidation processes (AOPs) and additional phenomena occurring during plasma treatment will also play a role in enhancing water quality [78], [79], [80], [81].

Regarding various essential reactive radicals and useful by-product substances in the PAMW generated through plasma-water-based nitrogen fixation at atmospheric pressure, it has been reported that nitrate is a more important form of nitrogen nutrient than ammonium form for duckweed (*Lemna minor* L.). The duckweed had the capacity to take up both forms of nitrogen nutrient  $\text{NO}_3^-$  and  $\text{NH}_4^+$  through both roots and fronds [82]. Based on the experimental results, it is evident that duckweed shows a greater affinity for absorbing nitrogen in the form of nitrate as opposed to ammonium.

While duckweed (*Lemna minor* L.) requires minimal phosphorus for optimal growth compared to nitrogen, it is nevertheless an essential nutrient. This study explores the use of domestic wastewater as a cost-effective source of phosphate, the preferred form of phosphorus uptake for duckweed. Although the phosphorus concentration in municipal wastewater after plasma treatment ranged from 0.33 mg/L to 0.37 mg/L, potentially lower than the optimal range of 4 to 22 mg/L for growth [3], the results suggest that even at this modest concentration, PAMW remains applicable and efficient for promoting the growth of duckweed.

The results also indicate that duckweed absorbed nitrogen nutrients in the form of nitrate more effectively than ammonium. Additionally, duckweed absorbed almost all phosphorus from PAMW for growth. Comparing this to Figure 7, the significant increase in the crude protein content of duckweed, including carotenoids, was associated with an increase

in nitrate uptake by duckweed. The reduction of ammonium and nitrite may be attributed to their conversion to nitrate through nitrification reactions by duckweed-associated bacteria [83]. It has been reported that at low concentrations, hydrogen peroxide, also present in PAMW, acts as a signaling molecule that can trigger various physiological responses in plants, such as stress responses, defense mechanisms, and cell elongation. This might lead to enhanced growth and development [84]. However, other long-lived substances dissolved in the PAMW used for duckweed cultivation, which has not been the focus of this study, could also contribute to the growth and nutritional content of duckweed via oxidative stress caused by ROS. Some of those substances are  $\text{OH}^-$ , nitric oxide (NO), and  $\text{O}_3$ , superoxide ( $\cdot\text{O}_2^-$ ) [85], [86].

This study has proposed the potential of PAMW as a medium for duckweed (*Lemna minor* L.) cultivation, with a primary focus on harnessing municipal wastewater to generate PAMW. Through the incorporation of AOPs during plasma treatment, essential plant macronutrients—N, P, and K—can be derived from key components present in wastewater, offering a comprehensive nutrient supply for agricultural applications. The designed atmospheric DC plasma model for wastewater treatment, driven by renewable solar energy, demonstrates promising results for large-scale production. Experimental findings indicate significant increases in nitrogen compounds and hydrogen peroxide, alongside and improve water quality post-treatment. In the constrain of this study, an increase in the number of anode modules could enhance all selected parameters. The primary purpose of the chosen plasma reactor is to transform atmospheric nitrogen into liquid nitrogen-based fertilizers for plants, while simultaneously improving the quality of community wastewater. Therefore, the reactor must be capable of producing reactive nitrogen species (RNS) like  $\text{NO}_x$ ,  $\text{HNO}_2$ , and  $\text{HNO}_3$ , which are essential for the production of nitrogen-based fertilizers, and reactive oxygen species (ROS) like  $\text{OH}$ ,  $\text{H}_2\text{O}_2$ , and  $\text{O}_3$ , which are essential for wastewater treatment. The performance of a plasma reactor in improving wastewater quality depends on several factors, including electrode configuration, working gas composition, discharge parameters (e.g., input power and discharge characteristics), type and initial concentration of pollutants, physical and chemical properties of wastewater (e.g., pH and electrical conductivity), volume of treated wastewater, and plasma exposure time [14], [87], [88].

Duckweed exhibits a preference for absorbing nitrogen in the form of nitrate over ammonium, while effectively utilizing phosphorus from PAMW for growth. These results underscore the potential of plasma-electrolysis treatment and its implications for sustainable agriculture, biofuel production, and food security. An in-depth investigation of the various reactive species generated by PAMW, coupled with physiological and biochemical analyses to assess potential biological effects on the plant, such as stress responses and long-term health consequences, could reveal additional benefits of PAMW for duckweed cultivation and beyond. Overall, the proposed plasma-electrolysis system presents a promising avenue for addressing wastewater treatment challenges while enhancing agricultural sustainability and food production.

Despite the potential of duckweed cultured in PAMW as a source of human food and animal feed, concerns regarding heavy metal bioaccumulation necessitate further investigation. Duckweed's documented proficiency in bioremediation through biological adsorption and intracellular accumulation of heavy metals from wastewater [89], [90] raises food safety questions. In order to address these concerns, it is essential to conduct a thorough assessment of the heavy metals present in PAMW before utilizing it as a culture medium. Furthermore, comprehensive evaluations of the food safety of a final product derived from duckweed are imperative before its consumption by humans or animals. During the early stages of development, using cultivated duckweed grown in PAMW as a biomass feedstock for biofuel production is a more suitable approach.

## 4 Conclusions

This study examined the effects of plasma-treated municipal wastewater on duckweed (*Lemna minor* L.). Using a solar-driven plasma-electrolysis reactor, contaminants in the wastewater were effectively degraded, reducing the COD value and producing nitrogen nutrients, particularly nitrate. The optimal treatment conditions were a discharge power of  $69.8 \pm 0.6$  W, a 1.00 cm discharge gap, and three anode modules, which significantly reduced COD values and increased nitrate, ammonium, and hydrogen peroxide production. Cultivating duckweed in this treated wastewater resulted in a 6.4-time increase in biomass after 7 days. The duckweed also showed significant increases in crude protein, carotenoid content, and chlorophyll compared to those grown in untreated





wastewater. These improvements were linked to higher nitrate and phosphate uptake from the treated water. In summary, plasma-treated municipal wastewater enhances duckweed growth and nutrient content, demonstrating its potential for sustainable agriculture.

### Acknowledgements

This research was funded by the Faculty of Science, Energy and Environment, King Mongkut's University of Technology North Bangkok, Rayong Campus (KMUTNB) with Contact No. SciEE-67-003. The authors also thank all staff members of Faculty of Science, Energy and Environment, KMUTNB, and Thailand Institute of Nuclear Technology (Public Organization) for their support.

### Author Contributions

S.U: conceptualization, research design, methodology, formal analysis and investigation, validation, writing an original draft, resources, supervision. M.J.: conceptualization, research design, methodology, formal analysis and investigation, validation, writing an original draft, resources, funding acquisition, supervision. K.P.: conceptualization, research design, methodology, formal analysis and investigation, validation, writing an original draft, resources, supervision. A.T.: conceptualization, resources. K.M.: conceptualization, formal analysis and investigation, validation, writing an original draft, writing—reviewing and editing. P.T.: conceptualization, research design, methodology, formal analysis and investigation, data curation, visualization, validation, writing an original draft, writing—reviewing and editing, resources, supervision, funding acquisition, project administration. All authors have read and agreed to the published version of the manuscript.

### Conflicts of Interest

The authors declare no conflict of interest.

### Declaration of generative AI and AI-assisted technologies in the writing process

During the preparation of this work, the authors used ChatGPT [chat.openai.com], Google Gemini [gemini.google.com], and QuillBot [quillbot.com] in order to improve only language and readability. After

using these tools/services, the authors reviewed and edited the content as needed and take full responsibility for the content of the publication.

### References

- [1] S. A. Hussain, F. Razi, K. Hewage, and R. Sadiq, "The perspective of energy poverty and 1st energy crisis of green transition," *Energy*, vol. 275, Jul. 2023, Art. no. 127487, doi: 10.1016/j.energy.2023.127487.
- [2] J. Geng, S. U. Haq, J. Abbas, H. Ye, P. Shahbaz, A. Abbas, and Y. Cai, "Survival in pandemic times: Managing energy efficiency, food diversity, and sustainable practices of nutrient intake amid COVID-19 crisis," *Frontiers in Environmental Science*, vol. 10, Jul. 2022, doi: 10.3389/fenvs.2022.945774.
- [3] J. Iqbal, A. Javed, and M. A. Baig, "Growth and nutrient removal efficiency of duckweed (*lemna minor*) from synthetic and dumpsite leachate under artificial and natural conditions," *PLOS ONE*, vol. 14, no. 8, Aug. 2019, Art. no. e0221755, doi: 10.1371/journal.pone.0221755.
- [4] H. Ullah, B. Gul, H. Khan, and U. Zeb, "Effect of salt stress on proximate composition of duckweed (*Lemna minor* L.)," *Heliyon*, vol. 7, no. 6, Jun. 2021, Art. no. e07399, doi: 10.1016/j.heliyon.2021.e07399.
- [5] L. Guo, J. Liu, Q. Wang, Y. Yang, Y. Yang, Q. Guo, H. Zhao, and W. Liu, "Evaluation of the potential of duckweed as a human food, bioethanol production feedstock, and antileukaemia drug," *Journal of Food Biochemistry*, vol. 2023, pp. 1–12, Mar. 2023, doi: 10.1155/2023/6065283.
- [6] J. Xu, Y. Shen, Y. Zheng, G. Smith, X. S. Sun, D. Wang, Y. Zhao, W. Zhang, and Y. Li, "Duckweed (Lemnaceae) for potentially nutritious human food: A review," *Food Reviews International*, vol. 39, no. 7, pp. 3620–3634, Aug. 2023, doi: 10.1080/87559129.2021.2012800.
- [7] X. Zhao, G. K. Moates, A. Elliston, D. R. Wilson, M. J. Coleman, and K. W. Waldron, "Simultaneous saccharification and fermentation of steam exploded duckweed: Improvement of the ethanol yield by increasing yeast titre," *Bioresource Technology*, vol. 194, pp. 263–269, Oct. 2015, doi: 10.1016/j.biortech.2015.06.131.
- [8] M. Krzywonos, Z. Romanowska-Duda, P. Seruga, B. Messyas, and S. Mec, "The use of

- plants from the lemnaceae family for biofuel production—A bibliometric and in-depth content analysis,” *Energies*, vol. 16, no. 4, Feb. 2023, Art. no. 2058, doi: 10.3390/en16042058.
- [9] X. Ge, N. Zhang, G. C. Phillips, and J. Xu, “Growing *Lemna minor* in agricultural wastewater and converting the duckweed biomass to ethanol,” *Bioresource Technology*, vol. 124, pp. 485–488, Nov. 2012, doi: 10.1016/j.biortech.2012.08.050.
- [10] D. Yadav, L. Barbora, D. Bora, S. Mitra, L. Rangan, and P. Mahanta, “An assessment of duckweed as a potential lignocellulosic feedstock for biogas production,” *International Biodeterioration & Biodegradation*, vol. 119, pp. 253–259, Apr. 2017, doi: 10.1016/j.ibiod.2016.09.007.
- [11] Y. Gao, K. Francis, and X. Zhang, “Review on formation of cold plasma activated water (PAW) and the applications in food and agriculture,” *Food Research International*, vol. 157, Jul. 2022, Art. no. 111246, doi: 10.1016/j.foodres.2022.111246.
- [12] A. Kumar, N. Škoro, W. Gernjak, and N. Puač, “Cold atmospheric plasma technology for removal of organic micropollutants from wastewater—A review,” *The European Physical Journal D*, vol. 75, no. 11, Nov. 2021, Art. no. 283, doi: 10.1140/epjd/s10053-021-00283-5.
- [13] R. Zhou, R. Zhou, P. Wang, Y. Xian, A. Mai-Prochnow, X. Lu, P. J. Cullen, K. (Ken) Ostrikov, and K. Bazaka, “Plasma-activated water: Generation, origin of reactive species and biological applications,” *Journal of Physics D: Applied Physics*, vol. 53, no. 30, Jul. 2020, Art. no. 303001, doi: 10.1088/1361-6463/ab81cf.
- [14] A. Barjasteh, Z. Dehghani, P. Lamichhane, N. Kaushik, E. H. Choi, and N. K. Kaushik, “Recent progress in applications of non-thermal plasma for water purification, bio-sterilization, and decontamination,” *Applied Sciences*, vol. 11, no. 8, Apr. 2021, Art. no. 3372, doi: 10.3390/app11083372.
- [15] K. Matra, W. Aryuwong, W. Meetang, S. Ruthairat, C. Dechthummarong, W. Sangwang, and V. Luang-In, “Application of electrical breakdown in liquid process on inulin structural transformations,” *IEEE Access*, vol. 11, pp. 114777–114789, 2023, doi: 10.1109/ACCESS.2023.3321339.
- [16] P. Poramapijitwat, P. Thana, P. Sukum, Y. Liangdeng, C. Kuensaen, and D. Boonyawan, “Selective cytotoxicity of lung cancer cells—A549 and H1299—Induced by Ringer’s lactate solution activated by a non-thermal air plasma jet device, Nightingale®,” *Plasma Chemistry and Plasma Processing*, vol. 43, no. 4, pp. 805–830, Jul. 2023, doi: 10.1007/s11090-023-10330-1.
- [17] P. Poramapijitwat, P. Thana, D. Boonyawan, K. Janpong, C. Kuensaen, W. Charentantanakul, L. D. Yu, and S. Sarapirom, “Effect of dielectric barrier discharge plasma jet on bactericidal and human dermal fibroblasts adult cells: In vitro contaminated wound healing model,” *Surface and Coatings Technology*, vol. 402, Nov. 2020, Art. no. 126482, doi: 10.1016/j.surfcoat.2020.126482.
- [18] K. Matra and S. Tawkaew, “Decolorization of methylene blue in an ar non-thermal plasma reactor,” *Journal of Engineering Science and Technology Review*, vol. 13, no. 1, pp. 114–119, Feb. 2020, doi: 10.25103/jestr.131.15.
- [19] S. A. A. Balkhi, S. M. Allabakshi, P. S. N. S. R. Srikar, S. Gomosta, R. K. Gangwar, and S. M. Maliyekkal, “Unwinding the correlation between atmospheric pressure plasma jet operating parameters and variation in antibiotic wastewater characteristics,” *Journal of Water Process Engineering*, vol. 60, Apr. 2024, Art. no. 105186, doi: 10.1016/j.jwpe.2024.105186.
- [20] S.-A. Yehia, N. Petrea, N. Grigoriu, S. Vizireanu, M. E. Zarif, L.G. Carpen, R.-E. Ginghina, and G. Dinescu, “Organophosphorus toxic compounds degradation in aqueous solutions using single filament dielectric barrier discharge plasma jet source,” *Journal of Water Process Engineering*, vol. 46, Apr. 2022, Art. no. 102637, doi: 10.1016/j.jwpe.2022.102637.
- [21] X. Hu, J. Feng, T. Ding, and R. Lv, “Correlation analysis of reactive oxygen and nitrogen species (RONS) components in plasma activated water (PAW) and its inactivation of *Bacillus cereus* endospore,” *Journal of Water Process Engineering*, vol. 56, Dec. 2023, Art. no. 104332, doi: 10.1016/j.jwpe.2023.104332.
- [22] Z. Xu, Y. Tang, S. Hu, Y. Lan, W. Xi, W. Han, D. Wu, F. Yang, and C. Cheng, “Inactivation of *Staphylococcus aureus* in water by dielectric barrier discharge plasma jet: The role of inorganic ions, organic matter, and turbidity,” *Journal of Water Process Engineering*, vol. 56, Dec. 2023, Art. no. 104449, doi: 10.1016/j.jwpe.2023.104449.



- [23] M. Zver, D. Dobnik, R. Zaplotnik, M. Mozetič, A. Filipić, and G. Primc, "Non-thermal plasma inactivation of viruses in water solutions," *Journal of Water Process Engineering*, vol. 53, Jul. 2023, Art. no. 103839, doi: 10.1016/j.jwpe.2023.103839.
- [24] R. P. Joshi and S. M. Thagard, "Streamer-like electrical discharges in water: Part II. environmental applications," *Plasma Chemistry and Plasma Processing*, vol. 33, no. 1, pp. 17–49, Feb. 2013, doi: 10.1007/s11090-013-9436-x.
- [25] A. Yusuf, H.K. Amusa, J.O. Eniola, A. Giwa, O. Pikuda, A. Dindi, and M. R. Bilad, "Hazardous and emerging contaminants removal from water by plasma-based treatment: A review of recent advances," *Chemical Engineering Journal Advances*, vol. 14, May 2023, Art. no. 100443, doi: 10.1016/j.ceja.2023.100443.
- [26] D. Boonyawan, K. Lamasai, C. Umongno, S. Rattanabattimong, L. D. Yu, C. Kuensaen, J. Maitip, and P. Thana, "Surface dielectric barrier discharge plasma-treated pork cut parts: Bactericidal efficacy and physiochemical characteristics," *Heliyon*, vol. 8, no. 10, Oct. 2022, Art. no. e10915, doi: 10.1016/j.heliyon.2022.e10915.
- [27] M. Pirsahab and N. Moradi, "Sonochemical degradation of pesticides in aqueous solution: Investigation on the influence of operating parameters and degradation pathway – A systematic review," *RSC Advances*, vol. 10, no. 13, pp. 7396–7423, 2020, doi: 10.1039/C9RA11025A.
- [28] E. M. Cuerda-Correa, M. F. Alexandre-Franco, and C. Fernández-González, "Advanced oxidation processes for the removal of antibiotics from water. An overview," *Water*, vol. 12, no. 1, Dec. 2019, Art. no. 102, doi: 10.3390/w12010102.
- [29] P. Gururani, P. Bhatnagar, B. Bisht, V. Kumar, N. C. Joshi, M. S. Tomar, and B. Pathak, "Cold plasma technology: Advanced and sustainable approach for wastewater treatment," *Environmental Science and Pollution Research*, vol. 28, no. 46, pp. 65062–65082, Dec. 2021, doi: 10.1007/s11356-021-16741-x.
- [30] S. Kesar and M. S. Bhatti, "Chlorination of secondary treated wastewater with sodium hypochlorite (NaOCl): An effective single alternate to other disinfectants," *Heliyon*, vol. 8, no. 11, Nov. 2022, Art. no. e11162, doi: 10.1016/j.heliyon.2022.e11162.
- [31] I. Zerva, N. Remmas, I. Kagalou, P. Melidis, M. Ariantsi, G. Sylaios, and S. Ntougias, "Effect of chlorination on microbiological quality of effluent of a full-scale wastewater treatment plant," *Life*, vol. 11, no. 1, Jan. 2021, Art. no. 68, doi: 10.3390/life11010068.
- [32] S. Theepharaksapan, Y. Lerkmahalikhit, P. Suwannapech, P. Boonnong, M. Limawatchanakarn, and K. Matra, "Impact of multi-air plasma jets on nitrogen concentration variance in effluent of membrane bioreactor pilot-plant," *Engineering and Applied Science Research*, vol. 48, no. 6, pp. 732–739, 2021, doi: 10.14456/easr.2021.75.
- [33] N. N. K. Kaushik, B. Ghimire, Y. Li, M. Adhikari, M. Veerana, N. N. K. Kaushik, N. Jha, B. Adhikari, S.-J. Lee, K. Masur, T. von Woedtke, K.-D. Weltmann, and E. H. Choi, "Biological and medical applications of plasma-activated media, water and solutions," *Biological Chemistry*, vol. 400, no. 1, pp. 39–62, Dec. 2018, doi: 10.1515/hsz-2018-0226.
- [34] S. Theepharaksapan, K. Matra, P. Thana, T. Traiporm, W. Aryuwong, Y. Tanakaran, Y. Lerkmahalikhit, L. Malun, and S. Ittisupornrat, "The potential of plasma-activated water as a liquid nitrogen fertilizer for microalgae cultivation," *IEEE Transactions on Plasma Science*, pp. 1–11, 2024, doi: 10.1109/TPS.2024.3362629.
- [35] S. Chuea-uan, D. Boonyawan, C. Sawangrat, and S. Thanapornpoonpong, "Using plasma-activated water generated by an air gliding arc as a nitrogen source for rice seed germination," *Agronomy*, vol. 14, no. 1, Dec. 2023, Art. no. 15, doi: 10.3390/agronomy14010015.
- [36] P. Lamichhane, R. Paneru, L. N. Nguyen, J. S. Lim, P. Bhartiya, B. C. Adhikari, S. Mumtaz, and E. H. Choi, "Plasma-assisted nitrogen fixation in water with various metals," *Reaction Chemistry & Engineering*, vol. 5, no. 11, pp. 2053–2057, 2020, doi: 10.1039/D0RE00248H.
- [37] N. Saksono, Harianingsih, B. Farawan, V. Luvita, and Z. Zakaria, "Reaction pathway of nitrate and ammonia formation in the plasma electrolysis process with nitrogen and oxygen gas injection," *Journal of Applied Electrochemistry*, vol. 53, no. 6, pp. 1183–1191, Jun. 2023, doi: 10.1007/s10800-023-01849-4.
- [38] H. Chen, D. Yuan, A. Wu, X. Lin, and X. Li, "Review of low-temperature plasma nitrogen

- fixation technology,” *Waste Disposal & Sustainable Energy*, vol. 3, no. 3, pp. 201–217, Sep. 2021, doi: 10.1007/s42768-021-00074-z.
- [39] N. Sarigul, F. Korkmaz, and İ. Kurultak, “A new artificial urine protocol to better imitate human urine,” *Scientific Reports*, vol. 9, no. 1, Dec. 2019, Art. no. 20159, doi: 10.1038/s41598-019-56693-4.
- [40] M. Qadir, P. Drechsel, B. J. Cisneros, Y. Kim, A. Pramanik, P. Mehta, and O. Olaniyan, “Global and regional potential of wastewater as a water, nutrient and energy source,” *Natural Resources Forum*, vol. 44, no. 1, pp. 40–51, Feb. 2020, doi: 10.1111/1477-8947.12187.
- [41] Y. Li, H. Li, X. Xu, S. Xiao, S. Wang, and S. Xu, “Fate of nitrogen in subsurface infiltration system for treating secondary effluent,” *Water Science and Engineering*, vol. 10, no. 3, pp. 217–224, Jul. 2017, doi: 10.1016/j.wse.2017.10.002.
- [42] J. Li, Q. Zhou, and L. C. Campos, “Removal of selected emerging PPCP compounds using greater duckweed (*Spirodela polyrhiza*) based lab-scale free water constructed wetland,” *Water Research*, vol. 126, pp. 252–261, Dec. 2017, doi: 10.1016/j.watres.2017.09.002.
- [43] S. Nakao, T. Nishio, and Y. Kanjo, “Simultaneous recovery of phosphorus and potassium as magnesium potassium phosphate from synthetic sewage sludge effluent,” *Environmental Technology*, vol. 38, no. 19, pp. 2416–2426, Oct. 2017, doi: 10.1080/09593330.2016.1264485.
- [44] P. J. Bruggeman, M. J. Kushner, B. R. Locke, J. G. E. Gardeniers, W. G. Graham, D. B. Graves, R. C. H. M. Hofman-Caris, D. Maric, J. P. Reid, E. Ceriani, D. F. Rivas, J. E. Foster, S. C. Garrick, Y. Gorbanev, S. Hamaguchi, F. Iza, H. Jablonowski, E. Klimova, J. Kolb, F. Krcma, P. Lukes, Z. Machala, I. Marinov, D. Mariotti, S. M. Thagard, D. Minakata, E. C. Neyts, J. Pawlat, Z. L. Petrovic, R. Pflieger, S. Reuter, D. C. Schram, S. Schröter, M. Shiraiwa, B. Tarabová, P. A. Tsai, J. R. R. Verlet, T. von Woedtke, K. R. Wilson, K. Yasui, and G. Zvereva, “Plasma–liquid interactions: A review and roadmap,” *Plasma Sources Science and Technology*, vol. 25, no. 5, Sep. 2016, Art. no. 053002, doi: 10.1088/0963-0252/25/5/053002.
- [45] K. Kosumsupamala, P. Thana, N. Palee, K. Lamasai, C. Kuensaen, A. Ngamjarurojana, P. Yangkhamman, and D. Boonyawan, “Air to H<sub>2</sub>-N<sub>2</sub> pulse plasma jet for in-vitro plant tissue culture process: Source characteristics,” *Plasma Chemistry and Plasma Processing*, vol. 42, no. 3, pp. 535–559, May 2022, doi: 10.1007/s11090-022-10228-4.
- [46] A. D. Eaton, L. S. Clesceri, E. W. Rice, and A. E. Greenberg, *Standard Methods for the Examination of Water & Wastewater*, 21st ed. Washington DC: American Public Health Association, 2005.
- [47] M. I. Fauth and A. C. Richardson, “Spectrophotometric determination of nitrogen dioxide in nitroglycerin,” *Microchemical Journal*, vol. 12, no. 4, pp. 534–541, Dec. 1967, doi: 10.1016/0026-265X(67)90091-4.
- [48] D. A. Cataldo, M. Maroon, L. E. Schrader, and V. L. Youngs, “Rapid colorimetric determination of nitrate in plant tissue by nitration of salicylic acid,” *Communications in Soil Science and Plant Analysis*, vol. 6, no. 1, pp. 71–80, Jan. 1975, doi: 10.1080/00103627509366547.
- [49] T. G. Towns, “Determination of aqueous phosphate by ascorbic acid reduction of phosphomolybdic acid,” *Analytical Chemistry*, vol. 58, no. 1, pp. 223–229, Jan. 1986, doi: 10.1021/ac00292a054.
- [50] L. Zhou and C. E. Boyd, “Comparison of Nessler, phenate, salicylate and ion selective electrode procedures for determination of total ammonia nitrogen in aquaculture,” *Aquaculture*, vol. 450, pp. 187–193, Jan. 2016, doi: 10.1016/j.aquaculture.2015.07.022.
- [51] P. Kundu, K. Anitha, and R. Niravath, “Feeding impact of the vegetable mite, tetranychus neocaledonicus andré (Acari: Tetranychidae) on *mentha rotundifolia* L.,” *International Journal of Recent Scientific Research*, vol. 7, no. 4, pp. 10406–10409, 2016.
- [52] AOAC, *Official Method of Analysis: Association of Analytical Chemists*, 19th ed. Washington DC: Association of Analytical Chemists, pp. 121–130, 2012.
- [53] K. Matra, H. Furuta, and A. Hatta, “Current-voltage characteristics of DC discharge in micro gas jet injected into vacuum environment,” *Journal of Physics: Conference Series*, vol. 441, 2013, Art. no. 012021, doi: 10.1088/1742-6596/441/1/012021.
- [54] K. Matra, “DC non-thermal atmospheric-pressure plasma jet generated using a syringe needle electrode,” *Japanese Journal of Applied Physics*, vol. 55, no. 7, 2016, doi: 10.7567/JJAP.55.07LB02.



- [55] P. Lu, D. Boehm, P. Bourke, and P. J. Cullen, "Achieving reactive species specificity within plasma-activated water through selective generation using air spark and glow discharges," *Plasma Processes and Polymers*, vol. 14, no. 8, Aug. 2017, doi: 10.1002/ppap.201600207.
- [56] V. A. Shakhatov and Yu. A. Lebedev, "Radiation spectroscopy in the study of the influence of a helium-nitrogen mixture composition on parameters of DC glow discharge and microwave discharge," *High Temperature*, vol. 50, no. 5, pp. 658–681, Sep. 2012, doi: 10.1134/S0018151X12050173.
- [57] P. Thana, A. Wijaikhum, P. Poramapijitwat, C. Kuensaen, J. Meerak, A. Ngamjarurojana, S. Sarapirom, and D. Boonyawan, "A compact pulse-modulation cold air plasma jet for the inactivation of chronic wound bacteria: development and characterization," *Heliyon*, vol. 5, no. 9, Sep. 2019, Art. no. e02455, doi: 10.1016/j.heliyon.2019.e02455.
- [58] J. Voráč, L. Kusýn, and P. Synek, "Deducing rotational quantum-state distributions from overlapping molecular spectra," *Review of Scientific Instruments*, vol. 90, no. 12, Dec. 2019, doi: 10.1063/1.5128455.
- [59] Q. Xiong, A. Y. Nikiforov, L. Li, P. Vanraes, N. Britun, R. Synders, X. P. Lu, and C. Leys, "Absolute OH density determination by laser induced fluorescence spectroscopy in an atmospheric pressure RF plasma jet," *The European Physical Journal D*, vol. 66, no. 11, Nov. 2012, Art. no. 281, doi: 10.1140/epjd/e2012-30474-8.
- [60] M. Mavadat, A. Ricard, C. Sarra-Bournet, and G. Laroche, "Determination of ro-vibrational excitations of N<sub>2</sub> (B, v') and N<sub>2</sub> (C, v') states in N<sub>2</sub> microwave discharges using visible and IR spectroscopy," *Journal of Physics D: Applied Physics*, vol. 44, no. 15, Apr. 2011, Art. no. 155207, doi: 10.1088/0022-3727/44/15/155207.
- [61] G. Cicala, E. D. Tommaso, A. C. Rainò, Y. A. Lebedev, and V. A. Shakhatov, "Study of positive column of glow discharge in nitrogen by optical emission spectroscopy and numerical simulation," *Plasma Sources Science and Technology*, vol. 18, no. 2, May 2009, Art. no. 025032, doi: 10.1088/0963-0252/18/2/025032.
- [62] T. Tian, H. Rabat, M. Magureanu, O. Aubry, and D. Hong, "Electrical investigation of a pin-to-plane dielectric barrier discharge in contact with water," *Journal of Applied Physics*, vol. 130, no. 11, Sep. 2021, doi: 10.1063/5.0056654.
- [63] S. B. Lyon, "Corrosion of Tungsten and its Alloys," in *Shreir's Corrosion*, Amsterdam, Netherlands: Elsevier, pp. 2151–2156, 2010, doi: 10.1016/B978-044452787-5.00105-0.
- [64] Z. Liu, J. C. Yang, J. Cao, and Y. Li, "Development and application of tungsten electrode materials," *Materials Science Forum*, vol. 817, pp. 348–354, Apr. 2015, doi: 10.4028/www.scientific.net/MSF.817.348.
- [65] F. Tochikubo, Y. Shimokawa, N. Shirai, and S. Uchida, "Chemical reactions in liquid induced by atmospheric-pressure dc glow discharge in contact with liquid," *Japanese Journal of Applied Physics*, vol. 53, no. 12, Dec. 2014, Art. no. 126201, doi: 10.7567/JJAP.53.126201.
- [66] P. Bruggeman and C. Leys, "Non-thermal plasmas in and in contact with liquids," *Journal of Physics D: Applied Physics*, vol. 42, no. 5, Mar. 2009, Art. no. 053001, doi: 10.1088/0022-3727/42/5/053001.
- [67] J. Liu, B. He, Q. Chen, J. Li, Q. Xiong, G. Yue, X. Zhang, S. Yang, H. Liu, and Q. H. Liu, "Direct synthesis of hydrogen peroxide from plasma-water interactions," *Scientific Reports*, vol. 6, no. 1, Dec. 2016, Art. no. 38454, doi: 10.1038/srep38454.
- [68] Z. Machala, B. Tarabová, D. Sersenová, M. Janda, and K. Hensel, "Chemical and antibacterial effects of plasma activated water: correlation with gaseous and aqueous reactive oxygen and nitrogen species, plasma sources and air flow conditions," *Journal of Physics D: Applied Physics*, vol. 52, no. 3, Jan. 2019, Art. no. 034002, doi: 10.1088/1361-6463/aae807.
- [69] P. Heirman, W. V. Boxem, and A. Bogaerts, "Reactivity and stability of plasma-generated oxygen and nitrogen species in buffered water solution: a computational study," *Physical Chemistry Chemical Physics*, vol. 21, no. 24, pp. 12881–12894, 2019, doi: 10.1039/C9CP00647H.
- [70] F. Rezaei, P. Vanraes, A. Nikiforov, R. Morent, and N. De Geyter, "Applications of plasma-liquid systems: A review," *Materials*, vol. 12, no. 17, Aug. 2019, Art. no. 2751, doi: 10.3390/ma12172751.
- [71] N. Bolouki, W.-H. Kuan, Y.-Y. Huang, and J.-H. Hsieh, "Characterizations of a plasma-water system generated by repetitive microsecond pulsed discharge with air, nitrogen, oxygen, and



- argon gases species,” *Applied Sciences*, vol. 11, no. 13, Jul. 2021, Art. no. 6158, doi: 10.3390/app11136158.
- [72] P. Lu, D. Boehm, P. Bourke, and P. J. Cullen, “Achieving reactive species specificity within plasma-activated water through selective generation using air spark and glow discharges,” *Plasma Processes and Polymers*, vol. 14, no. 8, Aug. 2017, doi: 10.1002/ppap.201600207.
- [73] H. Jablonowski, A. Schmidt-Bleker, K.-D. Weltmann, T. von Woedtke, and K. Wende, “Non-touching plasma–liquid interaction – where is aqueous nitric oxide generated?,” *Physical Chemistry Chemical Physics*, vol. 20, no. 39, pp. 25387–25398, 2018, doi: 10.1039/C8CP02412J.
- [74] H. Chen, D. Yuan, A. Wu, X. Lin, and X. Li, “Review of low-temperature plasma nitrogen fixation technology,” *Waste Disposal & Sustainable Energy*, vol. 3, no. 3, pp. 201–217, Sep. 2021, doi: 10.1007/s42768-021-00074-z.
- [75] P. Peng, P. Chen, M. Addy, Y. Cheng, Y. Zhang, E. Anderson, N. Zhou, C. Schiappacasse, R. Hatzenbeller, L. Fan, S. Liu, D. Chen, J. Liu, Y. Liu, and R. Ruan, “*In situ* plasma-assisted atmospheric nitrogen fixation using water and spray-type jet plasma,” *Chemical Communications*, vol. 54, no. 23, pp. 2886–2889, 2018, doi: 10.1039/C8CC00697K.
- [76] F. Judée, S. Simon, C. Bailly, and T. Dufour, “Plasma-activation of tap water using DBD for agronomy applications: Identification and quantification of long lifetime chemical species and production/consumption mechanisms,” *Water Research*, vol. 133, pp. 47–59, Apr. 2018, doi: 10.1016/j.watres.2017.12.035.
- [77] M. Ksibi, “Chemical oxidation with hydrogen peroxide for domestic wastewater treatment,” *Chemical Engineering Journal*, vol. 119, no. 2–3, pp. 161–165, Jun. 2006, doi: 10.1016/j.cej.2006.03.022.
- [78] S. Theepharakasapan and K. Matra, “Atmospheric argon plasma jet for post-treatment of Biotreated Landfill Leachate,” in *IEEECON 2018 - 6th International Electrical Engineering Congress*, 2018, doi: 10.1109/IEEECON.2018.8712320.
- [79] H. Gulyas, R. von Bismarck, and L. Hemmerling, “Treatment of industrial wastewaters with ozone/hydrogen peroxide,” *Water Science and Technology*, vol. 32, no. 7, pp. 127–134, 1995, doi: 10.1016/0273-1223(96)00056-X.
- [80] S. Horikoshi and N. Serpone, “In-liquid plasma: A novel tool in the fabrication of nanomaterials and in the treatment of wastewaters,” *RSC Advances*, vol. 7, no. 75, pp. 47196–47218, 2017, doi: 10.1039/c7ra09600c.
- [81] Y. Deng and R. Zhao, “Advanced oxidation processes (AOPs) in wastewater treatment,” *Current Pollution Reports*, vol. 1, pp. 167–176, Sep. 2015, doi: 10.1007/s40726-015-0015-z.
- [82] N. Cedergreen and T. V. Madsen, “Nitrogen uptake by the floating macrophyte *Lemna minor*,” *New Phytologist*, vol. 155, no. 2, pp. 285–292, Aug. 2002, doi: 10.1046/j.1469-8137.2002.00463.x.
- [83] N. J. Langenfeld, P. Kusuma, T. Wallentine, C. S. Criddle, L. C. Seefeldt, and B. Bugbee, “Optimizing nitrogen fixation and recycling for food production in regenerative life support systems,” *Frontiers in Astronomy and Space Sciences*, vol. 8, Jun. 2021, doi: 10.3389/fspas.2021.699688.
- [84] M. A. Hossain, S. Bhattacharjee, S.-M. Armin, P. Qian, W. Xin, H.-Y. Li, D.J. Burritt, M. Fujita, and L.-S. P. Tran, “Hydrogen peroxide priming modulates abiotic oxidative stress tolerance: insights from ROS detoxification and scavenging,” *Frontiers in Plant Science*, vol. 6, Jun. 2015, doi: 10.3389/fpls.2015.00420.
- [85] V. Stoleru, R. Burlica, G. Mihalache, D. Dirlau, S. Padureanu, G. C. Teliban, D. Astanei, A. Cojocar, O. Beniuga, and A. Patras, “Plant growth promotion effect of plasma activated water on *Lactuca sativa* L. cultivated in two different volumes of substrate,” *Scientific Reports*, vol. 10, no. 1, Dec. 2020, Art. no. 20920, doi: 10.1038/s41598-020-77355-w.
- [86] W. Li, C. H. Luna-Flores, R. Anangi, R. Zhou, X. Tan, M. Jessen, L. Liu, R. Zhou, T. Zhang, A. Gissibl, P. J. Cullen, K. (Ken) Ostrikov, and R. E. Speight, “Oxidative stress induced by plasma-activated water stimulates astaxanthin production in *Phaffia rhodozyma*,” *Bioresource Technology*, vol. 369, Feb. 2023, Art. no. 128370, doi: 10.1016/j.biortech.2022.128370.
- [87] N. Takeuchi and K. Yasuoka, “Review of plasma-based water treatment technologies for the decomposition of persistent organic compounds,” *Japanese Journal of Applied Physics*, vol. 60, no. SA, Jan. 2021, Art. no. SA0801, doi: 10.35848/1347-4065/abb75d.
- [88] H. Zeghioud, P. Nguyen-Tri, L. Khezami, A. Amrane, and A. A. Assadi, “Review on



- discharge Plasma for water treatment: mechanism, reactor geometries, active species and combined processes,” *Journal of Water Process Engineering*, vol. 38, Dec. 2020, Art. no. 101664, doi: 10.1016/j.jwpe.2020.101664.
- [89] Y. Zhou, A. Stepanenko, O. Kishchenko, J. Xu, and N. Borisjuk, “Duckweeds for phytoremediation of polluted water,” *Plants*, vol. 12, no. 3, Jan. 2023, Art. no. 589, doi: 10.3390/plants12030589.
- [90] M. K. Daud, S. Ali, Z. Abbas, I. E. Zaheer, M. A. Riaz, A. Malik, A. Hussain, M. Rizwan, M. Zia-ur-Rehman, and S. J. Zhu, “Potential of Duckweed (*Lemna minor*) for the Phytoremediation of Landfill Leachate,” *Journal of Chemistry*, vol. 2018, pp. 1–9, Dec. 2018, doi: 10.1155/2018/3951540.